Journal of the Serbian Chemical Society
JSCS-info@shd.org.rs • www.shd.org.rs/JSCS
J. Serb. Chem. Soc. 76 (8) 1153–1161 (2011) UDC 620.1+67.017:535.37:620.17:620.178
JSCS–4192 *Original scientific paper*

PMMA–Y_2O_3 (Eu^{3+}) nanocomposites: optical and mechanical properties

SALAH S. MUSBAH[1], VESNA J. RADOJEVIĆ[1]*, NADEŽDA V. BORNA[1], DUŠICA B. STOJANOVIĆ[1], MIROSLAV D. DRAMIĆANIN[2], ALEKSANDAR D. MARINKOVIĆ[1#] and RADOSLAV R. ALEKSIĆ[1]

[1]*Faculty of Technology and Metallurgy, University of Belgrade, Karnegijeva 4, Belgrade and* [2]*Institute of Nuclear Sciences "Vinča", P. O. Box 522, Belgrade, Serbia*

(Received 30 March 2010, revised 18 February 2011)

Abstract: The results of a study related to the processing and characterization of poly(methyl methacrylate) (PMMA)–Y_2O_3 (Eu^{3+}) nanocomposites are presented herein. The nanocomposite samples were prepared using a laboratory mixing molder with different contents of Eu-ion doped Y_2O_3 nanophosphor powder. The influence of particle content on the optical and dynamic mechanical properties of the nanocomposites was investigated. The intensity of the luminescence emission spectra increased as the nanophosphor content in the composite increased. The results of dynamic mechanical analysis revealed that the storage modulus, loss modulus and glass transition temperature (T_g) of the polymer composites increased with increasing content of the nanophosphor powder. The microhardness data also confirmed that the hardness number increased with nanoparticles concentration in the PMMA nanocomposites. The obtained results revealed a relatively linear relationship between T_g and the Vickers hardness.

Keywords: nanocomposites; luminescence; mechanical properties; dynamic mechanical analysis; microhardness.

INTRODUCTION

Nanocomposites are a distinct form of composite materials, which involve embedding nano- or molecular domain-sized particles into organic polymer, metal or ceramic matrix materials.[1,2] The intimate inclusion of nanoparticles in these matrices can greatly change the mechanical, electrical, optical or magnetic properties of these materials. The reason for this is that with such small in-

* Corresponding author. E-mail: vesnar@tmf.bg.ac.rs
# Serbian Chemical Society member.
doi: 10.2298/JSC100330094M

clusions, a large amount of interfacial phase material exists in the bulk of these nanocomposites.

This paper is related to the processing and characterization of polymer––nanophosphor composites, as promising materials for the production of nanocomposite fibers. Plastic optical fibers (POF) can be used for a number of applications, such as light transmission for signs and illumination, sensors and data communication.[3–5] Signal attenuation of commercial polymer fibers is much higher than that of glass fibers. In order to improve POF optical efficiency, research and processing are being developed in the direction of nanocomposite POF doped with dyes, and fluorescent or phosphorescent nanopowder.[6]

The optical properties of nano-sized phosphors are significantly improved in comparison to bulk materials (stronger luminescence emission and modified radiative lifetime).[7–20] Poly(methyl methacrylate), PMMA, nanocomposites containing Y_2O_3 doped with rare earths (RE) ions have been investigated and it was suggest that doped Y_2O_3 nanocrystals embedded in PMMA would have potential for various photonic applications, including laser systems and optical communication devices.[21,22] Nanocomposites PMMA–Y_2O_3:RE were successfully prepared by mixing Y_2O_3/Eu^{3+},Yb^{3+} or Y_2O_3/Eu^{3+} with PMMA for infrared cards.[22] The Eu-ion doped Y_2O_3 nanophosphor is useful for nanocomposite POF light guides because the luminescence wavelength of the Eu-ion (611 nm) is in the visible range of spectrum. It is very important to preserve their optical properties for a synergetic effect in functional nanocomposites.

In this work, Eu-ion doped Y_2O_3 nanophosphor powder was dispersed in PMMA as the host. The influence of the content of nanopowder on the optical properties, dynamic mechanical properties, transition temperature, T_g, and microhardness of the nanocomposites was investigated.

When an amorphous polymer is heated, it undergoes a phase transition from the glassy state to the rubbery state at the T_g, when abrupt jumps in the thermal expansion and heat capacity occur. The temperature coefficients of the molar volume, free volume and enthalpy change of the glass–rubber transition are closely related to the cohesive energy density of the polymer. The glass transition temperature, T_g is linearly related to the cohesive energy density (CED) by the following equation:[23]

$$T_g = (2E_C/mR) + C_1 \quad (1)$$

where E_C is the CED, T_g is the glass transition temperature (in K), m a parameter that describes the internal mobility of the groups in a single chain, R is the gas constant and C_1 is a constant. The CED is also the main factor determining hardness, H, which results in an almost linear relationship between T_g and H for a number of amorphous glassy polymers:[24–26]

$$H = kT_g + C \quad (2)$$

where *C* and *k* are experimental fitting parameters.

The nanoparticles penetrate into the polymer matrix and establish cohesive forces between the polymer chains and decrease the segmental mobility thereby increasing the T_g value.[27] Therefore, it is to be expected that the microhardness will also be increased. The expression for the Vickers hardness (*HV*) is:

$$HV = 1.854Pd^{-2} \quad (3)$$

where *P* is the applied load and *d* is the mean diagonal length of the diamond--shaped indent.

Dynamic mechanical analysis (DMA) is a sensitive technique that characterizes the mechanical response of materials by monitoring property change with respect to the temperature and frequency of an applied sinusoidal stress. This technique separates the dynamic response of materials in to two distinct parts: an elastic part (*E'*) – storage modulus and a viscous component (*E"*) – loss modulus. The loss factor, tan δ, is the ratio of the energy dissipated to the energy stored. The transition temperature (T_g) of a polymer is associated with the onset of the storage modulus – $T_{g(E')}$; the loss modulus peak – $T_{g(E")}$ and the tan δ peak – $T_{g(\tan \delta)}$. The onset of *E'* occurs first at the lowest temperature and relates to mechanical failure. The *E"* peak occurs next and is associated with the T_g as the temperature of the onset of segmental motion. The tan δ peak occurs at the highest temperature and represents a good measure of the "leather like" midpoint between the glassy and rubbery state.[28,29]

EXPERIMENTAL

The nanopowder was synthesized by a complex polymer solution method (PCS), employing poly(ethylene glycol) (PEG) fuel. The particle size was about 30–40 nm.[30]

The nanocomposites were prepared by melt compounding in a Laboratory Mixing Molder (Atlas, USA), at a working temperature of 250 °C and a rotor speed of 180 rpm for 20 min. The polymer component of the composite was extrusion grade PMMA pellets, Acryrex® CM-205, Chi Mei Corporation, Taiwan. Samples with different contents of (Eu^{3+})Y_2O_3 powder: 0.1, 0.5, 1.0 and 1.5 % by weight were processed.

The infrared (IR) spectra of the powder, pure PMMA and the composites were obtained by Fourier transform infrared (FT-IR) spectroscopy (Hartmann & Braun, MB-series) in KBr discs. The scanning range was between 4000 and 400 cm^{-1} with a resolution of 4 cm^{-1}.

The emission spectra of the PMMA-Y_2O_3 (Eu^{3+}) nanocomposites were collected at room temperature after excitation into the $^7F_0 \rightarrow {}^5D_2$ absorption band. The excitation source was an Optical Parametric Oscillator (O.P.O.) pumped by the third harmonic of an Nd:YAG laser. The emission was analyzed using an HR250 monochromator (Jobin-Yvon) and then detected by an ICCD camera (Princeton Instrument).

The microhardness measurements were performed at the room temperature using a Vickers microhardness tester Leitz, Kleinharteprufer Durimet I. The Vickers microhardness test uses a square based pyramidal indenter with an apex of $\alpha = 136°$, producing a diamond-shaped indent on the surface. A press load of 490 mN, a press time of 15 s, and a holding time of 5 s after completing the indentation were used. Individual Vickers microhardness values (*HV*) were calculated as the mean value of at least five indentations.

A dynamic mechanical analysis (DMA) instrument (TA Instruments Q800) was used to determine the dynamic mechanical properties of the samples. The experiments were realized in the single-cantilever mode over a temperature range from 25 to 160 °C at a fixed frequency of 1 Hz. The heating ramp rate was 3 °C min^{-1}. The temperature dependence of the storage modulus, loss modulus and tan δ were obtained.

RESULTS AND DISCUSSION

The FT-IR transmission spectra of the powder, PMMA and composites are illustrated in Fig. 1. The peaks at 2946 and 1735 cm^{-1} are assigned to C–H and C=O stretching vibrations in PMMA, respectively. The absorption bands of PMMA (1439, 840, 750 and 440 cm^{-1}), and the vibration bands of PMMA (3458, 1385, 1133 and 974 cm^{-1}), were observed in the spectra. In the spectrum of Y_2O_3 (Eu^{3+}), the transmission band centered at 560 cm^{-1} is attributed to Y–O lattice vibrations. This peak also appeared in all the spectra of all the composites.

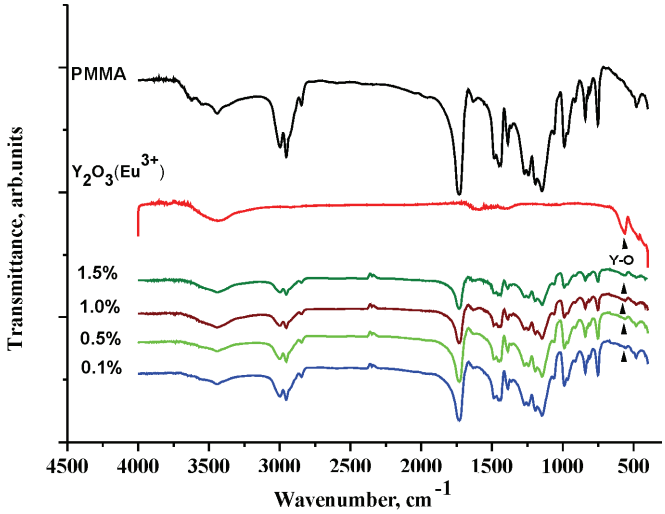

Fig. 1. FT-IR Spectra of Y_2O_3 (Eu^{3+}), PMMA and the composites with different contents of Y_2O_3 (Eu^{3+}).

The emission luminescence spectra of nanocomposite are presented in Fig. 2. The spectra exhibit groups of distinctive emission peaks in the 580–711 nm range. These emission peaks can be related to each of the $^5D_0 \rightarrow {}^7FJ$ (J = 0, 1, 2, 3 or 4) transitions of Eu^{3+}, which are characteristic for Eu^{3+} within a crystallized cubic phase. The strongest emission peak at 611 nm is caused by the electron dipole transition of Eu^{3+} ($^5D_0 \rightarrow {}^7F_2$), corresponding to the red luminescence. The intensity of the emission peak increased with increasing powder content in composite. It is very important that the nano-phosphors maintain their optical properties in the composites. The strongest emission peak at 611 nm was obtained in the range of wavelengths where the maximum signal attenuation of

PMMA optical fiber is expected to be found. This feature will improve the transmission properties of POF and will prolong the length of a light guide.

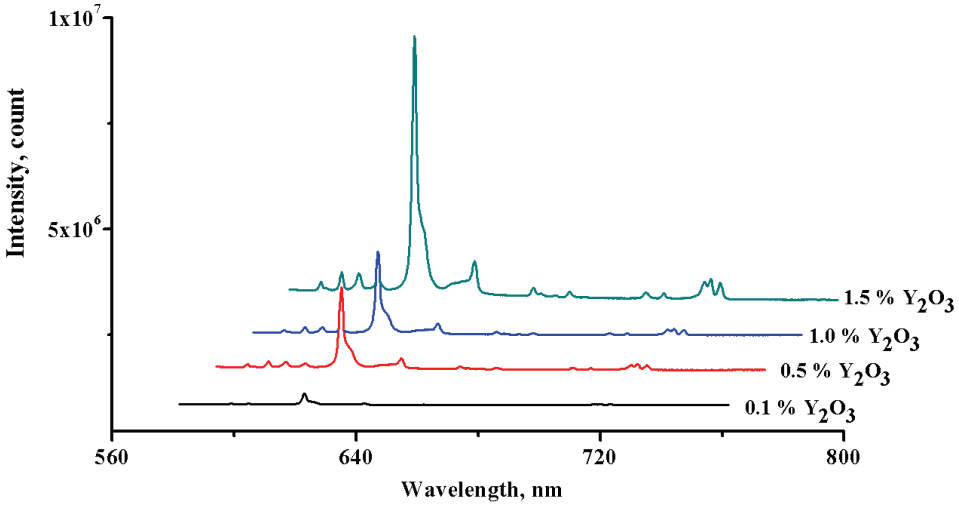

Fig. 2. Emission spectra of the PMMA–Y_2O_3 (Eu^{3+}) nanocomposites at room temperature.

Investigations of the dynamic mechanical properties of the samples provided information on the transitions occurring in the materials (Fig. 3). The DMA results revealed that the storage modulus of the all the composite samples were higher than that of a pure PMMA at 30 °C (Table I). The increase of nanopowder content up to 1 % increased the storage modulus of composite by 15.5 % compared to that of pure PMMA. With 1.5 % of the nanophosphor, the storage modulus of the composite was only 5.1 % higher than that of PMMA, because of agglomeration of the nanoparticles. The corresponding loss moduli were between 175 and 200 MPa and obviously increased with increasing content of nanopowder in the same manner as the storage modulus. The T_g values of the PMMA–$-Y_2O_3$ (Eu^{3+}) composites were also higher than that of PMMA and increased with increasing content of the nanoparticles. The results suggested that the nanoparticles did not disperse individually but as aggregates; however, notable increases in the glass transition temperature in the order of 2 to 8 °C were evidenced.

The hardness (H) of a material is a measure of its resistance to shear stresses under local volume compression. The hardness number increased with Y_2O_3 (Eu^{3+}) concentration in the PMMA nanocomposites. The increased resistance to surface deformation of the PMMA nanocomposites may be due to a decrease in the free volume of the matrix associated with the formation of apparent physical cross-linking and entanglements. The T_g is linearly related to the microhardness

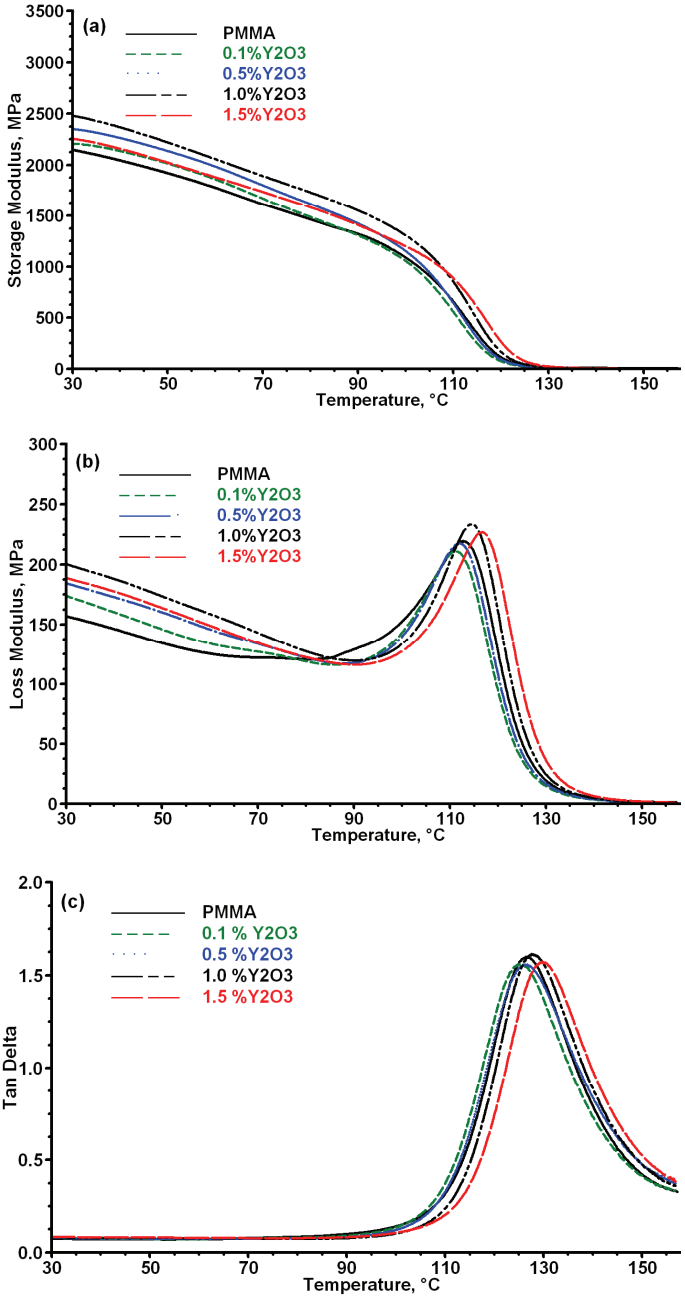

Fig. 3. Temperature dependence of a) the storage modulus, b) the loss modulus and c) tan δ for composites with different contents of Y_2O_3 (Eu^{3+}).

TABLE I. Results of DMA: *E*' and *E*" at 30 °C, values of T_g obtained by *E*' onset, *E*" maximum, tan δ maximum and microhardness (*HV*)

$c_{Y_2O_3}$ / %	*E*' / MPa	Δ*E*' / %	*E*" / MPa	$T_{g(E')}$ / °C,	$T_{g(E")}$ / °C	$T_{g(\tan\delta)}$ / °C	*HV* / MPa
0	2147	–	156.9	100.68	112.70	126.40	254.87
0.1	2199	2.4	175.0	102.05	111.33	125.48	259.256
0.5	2352	9.5	184.6	103.29	111.84	126.20	269.812
1.0	2481	15.5	200.6	105.71	114.44	127.60	276.631
1.5	2256	5.1	189.0	108.47	116.73	129.70	280.139

according to Eq. (2). The correlations between *HV* and the T_g derived from the DMA curves by the *E*' onset, by the *E*" peak and by the tan δ peak are presented in Fig. 4. The fitting coefficients of these correlations, *C*, *k* and R^2 are presented in Table II for all three lines. The value of R^2 of the linear correlation between *HV* and $T_{g(E')}$ is the highest. This means that the *E*' onset is the most sensitive to local shear stresses and it exhibits the best linearity with microhardness.

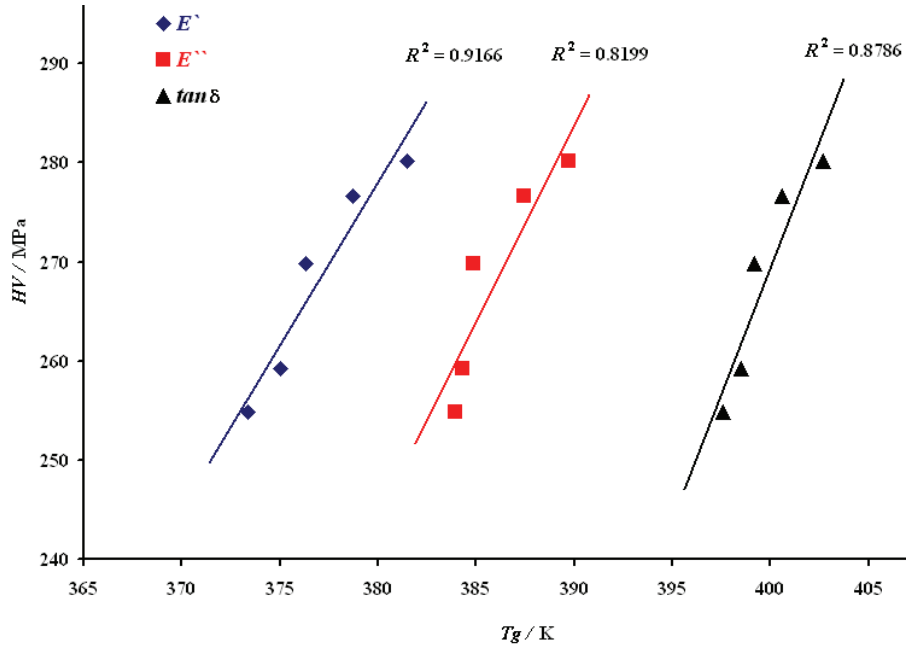

Fig. 4. Linear correlations of *HV* and T_g obtained from the DMA results – $T_{g(E')}$, $T_{g\,(E")}$ and $T_{g(\tan\delta)}$

TABLE II. Fitting parameters of the T_g–*HV* correlations

Fitting parameter	$HV - T_{g(E')}$	$HV - T_{g(E")}$	$HV - T_{g(\tan\delta)}$
C / MPa	–969.28	–1272.6	–1773.6
k / MPa K^{-1}	3.2825	3.9911	5.108
R^2	0.9166	0.8199	0.8786

CONCLUSIONS

The optical and mechanical properties of PMMA–Y_2O_3 (Eu^{3+}) nanocomposites were investigated. The luminescence spectra of the nanocomposites revealed that the phosphorescence of the powder remained on compositing and the emission intensity was enhanced as the content of the powder in the composites increased. The results obtained from the DMA showed that on the addition of nanopowder, the T_g of the PMMA increased, but only by a few degrees; this also suggests that the nanoparticles did not disperse individually but as aggregates. The microhardness number increased with increasing Y_2O_3 (Eu^{3+}) content in the PMMA nanocomposites. A nearly linear correlation between T_g and microhardness was obtained, because both properties are closely related to the cohesive energy density. This result is in accordance with previously reported results for amorphous glassy polymers, and now this linear correlation is applicable to similar composite configurations.

Acknowledgement. This work was supported by the Ministry of Education and Science of the Republic of Serbia, Project No. TR 19047.

И З В О Д

НАНОКОМПОЗИТ PMMA–Y_2O_3 (Eu^{3+}): ОПТИЧКА И МЕХАНИЧКА СВОЈСТВА

SALAH S. MUSBAH[1], ВЕСНА Ј. РАДОЈЕВИЋ[1], НАДЕЖДА В. БОРНА[1], ДУШИЦА Б. СТОЈАНОВИЋ[1], МИРОСЛАВ ДРАМИЋАНИН[2], АЛЕКСАНДАР Д. МАРИНКОВИЋ[1] и РАДОСЛАВ Р. АЛЕКСИЋ[1]

[1]*Технолошко–металуршки факултет, Универзитет у Београду,, Карнегијева 4, Београд и*
[2]*Институт за нуклеарне науке "Винча", п. пр. 522, Београд*

У оквиру овог рада презентовано је истраживање процесирања и карактеризације нанокомпозитног материјала поли(метил-метакрилат) (PMMA)–Y_2O_3 (Eu^{3+}). Узорци са различитим садржајем нанофосфора Y_2O_3 допираног са Eu јонима процесирани су у лабораторијском уређају за умешавање термопластичних полимера. Испитиван је утицај удела наночестица на оптичка и динамичко–механичка својства композита. Интензитет луминисцентног емисионог спектра композита расте са уделом нанофосфора. Резултати DMA показују да модул депоноване енергије, модул губитака и температура трансформације расту са повећањем удела наночестица. Микротврдоћа композита такође расте са повећањем удела наночестица у композиту и показује скоро линеарну зависност од температуре трансформације (T_g).

(Примљено 30. марта 2010, ревидирано 18. фебруара 2011)

REFERENCES

1. D. R. Paul, L. M. Robeson, *Polymer* **49** (2008) 3187
2. S. C. Tjong, *Mater. Sci. Eng., R* **53** (2006) 73
3. Y. Osada, D. E. D. Rossi, *Polymer Sensors and Actuators*, Springer-Verlag, Heidelberg, Germany, 2000
4. S. M. Vaezi-Nejad, *Selected Topics in Advanced Solid State and Fiber Optic Sensors*, IEE, London, UK, 2000

5. R. J. Bartlett, R. Philip-Chandy, P. Eldridge, D. F. Merchant, R. Morgan, P. J. Scully, *Trans. Inst. Meas. Control* **22** (2000) 431
6. K. Mohomed, T. G. Gerasimov, H. Abourahma, M. J. Zaworotko, J. P. Harmon, *Mater. Sci. Eng., A* **409** (2005) 227
7. H. Eilers, B. M. Tissue, *Chem. Phys. Lett.* **251** (1996) 74
8. B. Bihari, H. Eilers, B. M. Tissue, *J. Lumin.* **75** (1997) 1
9. T. Ye, Z. Guiwen, Z. Weiping, X. Shangda, *Mater. Res. Bull*. **32** (1997) 501
10. Q. Li, L. Gao, D. Yan, *Nanostruct. Mater*. **8** (1997) 825
11. D. K. Williams, B. Bihari, B. M. Tissue, J. M. McHale, *J. Phys. Chem., B* **102** (1998) 916
12. A. Konrad, T. Fries, A. Gahn, F. Kummer, U. Herr, R. Tidecks, K. Samwer *J. Appl. Phys.* **86** (1999) 3129
13. T. Igarashi, M. Ihara, T. Kusunoki, K. Ohno, T. Isobe, M. Senna, *Appl. Phys. Lett.* **76** (2000) 1549
14. G. Wakefield, E. Holland, P. J. Dobson, J. L. Hutchison, *Adv. Mat*. **13** (2001) 1557
15. D. Matsuura, *Appl. Phys. Lett.* **81** (2002) 4526
16. T. L. Phan, M. H. Phan, N. Vu, T. K. Anh, S.-C. Yu, *Phys. Status Solidi, A* **201** (2004) 2170
17. N. Nguyen, M. H. Nam, T. K. Anh, L. Q. Minh, and E. Tanguy *Adv. Nat. Sci*. **6** (2006) 119
18. N. Vu, T. K. Anh, G.-C. Yi, W. Strek, *J. Lumin.* **122**–**123** (2007) 776
19. E. Ritzhaupt-Kleissl, J. Boehm , J. Hausselt, T. Hanemann, *Mater. Sci. Eng., C* **26** (2006) 1067
20. T. K. Anh, N. Vu, M. H. Nam, L. Q. Minh, *Adv. Nat. Sci.* **7** (2006) 63
21. K. S. Dhiraj, S. Chandra, J. B. Gruber, W. Gorski, M. Zhang, J. H. Shim, *J. Appl. Phys.* **105** (2009) 093105
22. T. K. Anh, P. Benalloul, C. Barthou, L. T. K. Giang, N. Vu, L. Q. Minh, *J. Nanomaterials* (2007) 2
23. B. Crist, in *Materials Science and Technology*, Vol. 1, E. L. Thomas, Ed., VCH, Weinheim, Germany, 1993, p. 427
24. F. J. Baltá-Calleja, A. Flores, F. Ania, in *Mechanical properties of polymers based on nanostructure and morphology*, G. H. Michler, F. J. Baltá-Calleja, Eds., Taylor and Francis, London, UK, 2005, p. 285
25. A. Flores, F. Ania, F. J. Baltá-Calleja, *Polymer* **50** (2009) 729
26. S. Fakirov, F. J. Balta-Calleja, M. Krumova, *J. Polym. Sci., B* **37** (1999) 1413
27. A. K. Adiyodi, X. Joseph, P. V. Jyithy, G. Jose, N. V. Unnikrishnan, *Materials Science – Poland* **27** (2009) 297
28. E. A. Turi, *Thermal Characterization of Polymeric Materials*, Vol. I, 2nd ed., Academic Press, New York, 1997, p. 980
29. M. Dixit, S. Gupta, V. Mathur, K. S. Rathore, K. Sharma, N. S. Saxena, *Chalcogenide Lett.* **6** (2009) 131
30. Z. Antic, R. Krsmanovic, I. Zekovic, M. D. Dramicanin, in *Proceeding of Electro-ceramics XI*, (2008), University of Manchester, Manchester, UK, Abstracts and CD proceedings, 2008, C-038-P.